Abdominal Lymph Node Anatomy

3

Amreen Shakur, Aileen O'Shea,
and Mukesh G. Harisinghani

Lymph node metastasis is frequently seen in most primary abdominal malignant tumors. The tumor cells enter lymphatic vessels and travel to the lymph nodes along lymphatic drainage pathways. The lymphatic vessels and lymph nodes generally accompany the blood vessels supplying or draining the organs. They are all located in the subperitoneal space within the ligaments, mesentery, mesocolon, and extra peritoneum. Metastasis to the lymph nodes generally follows the nodal station in a stepwise direction—that is, from the primary tumor to the nodal station that is closest to the primary tumor and then progresses farther away but within the lymphatic drainage pathways. Metastasis to a nodal station that is farther from the primary tumor without involving the nodal station close to the primary tumor ("skip" metastasis) is rare. The key to understanding the pathways of lymphatic drainage of each individual organ is to understand the ligamentous, mesenteric, and peritoneal attachments and the vascular supply of that organ [1].

The benefits of understanding the pathways of lymphatic drainage of each individual organ are threefold. First, when the site of the primary tumor is known, it allows identification of the expected first landing site for nodal metastases by following the vascular supply to that organ [2, 3]. Second, when the primary site of tumor is not clinically known, identifying abnormal nodes in certain locations allows tracking the arterial supply or venous drainage in that region to the primary organ. Third, it also allows identification of the expected site of recurrent disease or nodal metastasis or the pattern of disease progression after treatment by looking at the nodal station beyond the treated site. The location of drainage pattern of abdominal lymphatics is outlined in Table 3.1.

The accuracy for characterizing malignant lymph nodes based on size criteria (Table 3.2) is low and has been described in published reports.

A. Shakur · A. O'Shea · M. G. Harisinghani (✉)
Department of Radiology, Massachusetts General Hospital, Harvard Medical School, Boston, MA, USA
e-mail: mharisinghani@mgh.harvard.edu

M. G. Harisinghani (ed.), *Atlas of Lymph Node Anatomy*,
https://doi.org/10.1007/978-3-030-80899-0_3

Normal-sized lymph nodes can be malignant, and enlarged lymph nodes can be nonmalignant (see Fig. 3.1) [6–8]. Newer imaging technology involving novel MRI lymphotropic contrast agents such as ferumoxtran-10 and ferumoxytol has shown to be superior in discriminating the two [9]. These nanoparticles target the reticuloendothelial system and are carried into lymph nodes by macrophages and cause a prolonged shortening of both T2 and T2*. Normal lymph nodes contain large numbers of macrophages, whereas in metastatic nodes, there is a relative absence resulting in signal hyperintensity on MR [10].

The use of PET-CT is well established in certain cancer subtypes. For example, in esophageal and anal cancers, it is an important tool in the diagnostic workup. In colorectal cancer and to a lesser degree in localized gastric and pancreatic cancers, PET-CT is helpful in detecting distant metastases [11–13].

Table 3.1 Lymphatics of the abdomen [4]

Structure	Location	Afferents from	Efferents to	Regions drained	Notes
Paracardial nodes	Around the esophagogastric junction	Lymphatic vessels of the fundus and cardia of the stomach	Left gastric nodes	Fundus and cardia of the stomach	Paracardial nodes are 5 or 6 in number
Gastric nodes, left	On the lesser curvature of the stomach, along the course of the left gastric vessels	Lymphatic vessels from the lesser curvature of the stomach	Celiac nodes	Lesser curvature of the stomach	Left gastric nodes are 10–20 in number
Gastric nodes, right	On the lesser curvature of the stomach, along the course of the right gastric vessels	Lymphatic vessels from the lesser curvature of the stomach	Celiac nodes	Lesser curvature of the stomach	Right gastric nodes are 2–3 in number
Gastro-omental nodes, left	On the greater curvature of the stomach, along the left gastro-omental vessels	Lymphatic vessels from the greater curvature of the stomach	Splenic nodes	Left half of the greater curvature of the stomach	Left gastro-omental nodes are 1 or 2 in number
Gastro-omental nodes, right	On the greater curvature of the stomach, along the right gastro-omental vessels	Lymphatic vessels from the greater curvature of the stomach	Pyloric nodes	Greater curvature of the stomach	Right gastro-omental nodes are 6–12 in number
Hepatic nodes	Along the course of the common hepatic artery	Right gastric nodes, pyloric nodes	Celiac nodes	Liver and gall bladder; extrahepatic biliary apparatus; respiratory diaphragm; head of pancreas and duodenum	Hepatic nodes drain a portion of the respiratory diaphragm because of the common embryonic origin of the diaphragm and the liver (septum transversum)
Cystic node	Near the neck of the gall bladder	Lymphatic vessels of the gall bladder	Hepatic nodes	Gallbladder	Cystic node drains to the node of the omental foramen, then to hepatic nodes
Pyloric nodes	Near the termination of the gastroduodenal artery.	Pancreaticoduodenal nodes	Hepatic nodes	Head of pancreas and duodenum; right half of greater curvature of stomach	Pyloric nodes are 6–8 in number

(continued)

Table 3.1 (continued)

Structure	Location	Afferents from	Efferents to	Regions drained	Notes
Pancreaticoduodenal nodes	Along the pancreaticoduodenal arcade of vessels	Lymphatic vessels from the duodenum and pancreas	Pyloric nodes	Duodenum and head of the pancreas	Lymph from the pancreas is drained in three different directions: pancreaticoduodenal nodes, pancreaticosplenic nodes, superior mesenteric nodes
Pancreaticosplenic nodes	Along the splenic vessels	Lymphatic vessels from the pancreas and greater curvature of the stomach	Celiac nodes	Neck, body, and tail of the pancreas; left half of the greater curvature of the stomach	Lymph from the pancreas is drained in three different directions: pancreaticoduodenal nodes, pancreaticosplenic nodes, superior mesenteric nodes
Celiac nodes	Around the celiac arterial trunk	Hepatic nodes, gastric nodes, pancreaticosplenic nodes	Intestinal lymph trunk	Liver, gall bladder, stomach, spleen, pancreas	Celiac nodes are 3–6 in number
Mesenteric nodes	Along the vasa recta and branches of the superior mesenteric a. Between the leaves of peritoneum forming the mesentery	Peripheral nodes located along the attachment of the mesentery	Superior mesenteric nodes	Small intestine	Mesenteric nodes may number as many as 200; an important node group in cases of intestinal cancer
Mesenteric nodes, superior	Along the course of the superior mesenteric artery	Mesenteric nodes, ileocolic nodes, right colic nodes, middle colic nodes	Celiac nodes, intestinal lymph trunk	Gut and viscera supplied by the superior mesenteric artery	Superior mesenteric nodes are important in the spread of cancer from the small and large intestine
Inferior mesenteric nodes	Around the root of the inferior mesenteric artery.	Peripheral nodes located along the marginal artery.	Lumbar chain of nodes, superior mesenteric nodes	Distal one-third of the transverse colon, descending colon, sigmoid colon, rectum	Inferior mesenteric nodes may number as high as 90; an important node group in cases of cancer of the colon and rectum

Ileocolic nodes	Along the origin and terminal end of the ileocolic vessels	Peripheral nodes located along the attachment of the mesentery	Superior mesenteric nodes	Ileum, cecum, appendix	Ileocolic nodes located near the ileocecal junction may be divided into two subsidiary groups: cecal nodes and appendicular nodes
Colic nodes, right	Along the course of the right colic vessels	Peripheral nodes located along the marginal artery	Superior mesenteric nodes	Ascending colon, cecum	Right colic nodes are approximately 70 in number
Colic nodes, middle	Along the course of the middle colic vessels	Peripheral nodes located along the attachment of the mesentery	Superior mesenteric nodes	Transverse colon	Middle colic nodes are approximately 40 in number
Colic nodes, left	Along the course of the left colic vessels	Peripheral nodes located along the marginal artery	Inferior mesenteric nodes	Descending colon, sigmoid	Left colic nodes are approximately 30 in number
Pararectal nodes	Along the course of the superior rectal vessels	Lymphatic vessels from the rectum and anal canal	Inferior mesenteric nodes	Rectum and anal canal	Pararectal nodes are small lymph nodes that are not well localized
Lateral aortic nodes	Along the inferior vena cava and abdominal aorta from the aortic bifurcation to the aortic hiatus of the diaphragm	Common iliac nodes; lymphatic vessels from the posterior abdominal wall and viscera	Efferents form one lumbar trunk on each side	Lower limb; pelvic organs; perineum; anterior and posterior abdominal wall; kidney; suprarenal gland; respiratory diaphragm	Also known as lumbar nodes; the intestinal trunk drains into to the left lumbar trunk; the lumbar trunks unite to form the thoracic duct/cisterna chili

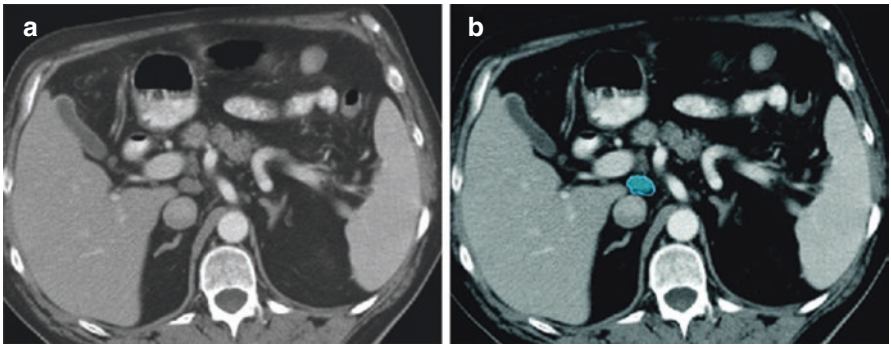

Fig. 3.1 (**a**, **b**) Axial CT image in a patient with cirrhosis shows a prominent portocaval lymph node (blue)

3.1 Lymphatic Spread of Malignancies

3.1.1 Liver

Hepatocellular carcinoma (HCC) is the most common primary visceral malignancy [14]. Lymph node metastases (LNM) are rare and generally associated with poor prognosis in hepatocellular carcinoma (see Fig. 3.2). The median survival time of patients with single and multiple LNM after surgery was 52 and 14 months, respectively [15].

Table 3.4 outlines the regional lymph nodes for hepatocellular carcinoma. There are several potential pathways for tumor spread, including superficial and deep pathways, below and above the diaphragm. The superficial lymphatic network (see Fig. 3.3) is extensive and is located beneath Glisson's capsule. The drainage of superficial lymphatics can be classified into three major groups:

1. Through the hepatoduodenal and gastrohepatic ligament pathway, it is the most common distribution of lymph node metastasis.
2. The diaphragmatic lymphatic plexus is another important pathway of drainage because a large portion of the liver is in contact with the diaphragm either directly at the bare area or indirectly through the coronary and triangular ligaments. However, nodal metastasis through this pathway is often overlooked.
3. The rare pathway for nodal metastasis is along the falciform ligament to the deep superior epigastric node in the anterior abdominal wall along the deep superior epigastric artery below the xiphoid cartilage.

The deep lymphatic network follows the portal veins, drains into the lymph nodes at the hilum of the liver, the hepatic lymph nodes, then to the nodes in the hepatoduodenal ligament. The nodes in the hepatoduodenal ligament can be separated into two major chains: the hepatic artery chain and posterior periportal chain (see Figs. 3.4 and 3.5). The hepatic artery chain follows the common hepatic artery to the node at the celiac axis and then into the cisterna chyli. The posterior periportal chain is located posterior to the portal vein in the hepatoduodenal ligament (see

Fig. 3.6). It drains into the retropancreatic nodes and the aortocaval node (see Fig. 3.7) and then into the cisterna chyli and the thoracic duct [1].

Tables 3.3 and 3.4 list the N staging for hepatocellular carcinoma and the regional lymph nodes for hepatocellular carcinoma. Nodal metastases have been identified as the main risk factor in the overall survival in patients with HCC with extrahepatic metastases, with an overall survival of nearly 3 months without treatment [16, 17]. Surgical management provides the best long-term survival; however, only approximately 20% of patients are surgical candidates at diagnosis [18]. Regional lymph node involvement is a contraindication for resection and no consensus has yet been reached on the treatment strategy for LNM from HCC. Long-term survival can be expected after selective lymphadenectomy, especially in patients with a single LNM. On the other hand, efficacy of selective lymphadenectomy for multiple LNM seemed equivocal due to its advanced and systemic nature of the disease [3]. Nonsurgical therapies aiming to achieve local control for patients ineligible for curative therapy include transarterial chemoembolization (TACE). External beam radiation therapy (EBRT) has been limited to the palliation of HCC metastases associated with distressing symptoms [19]. Radiofrequency ablation, although often used with curative intent for the primary tumor has also shown to be beneficial in treating HCC oligometastases [17, 20].

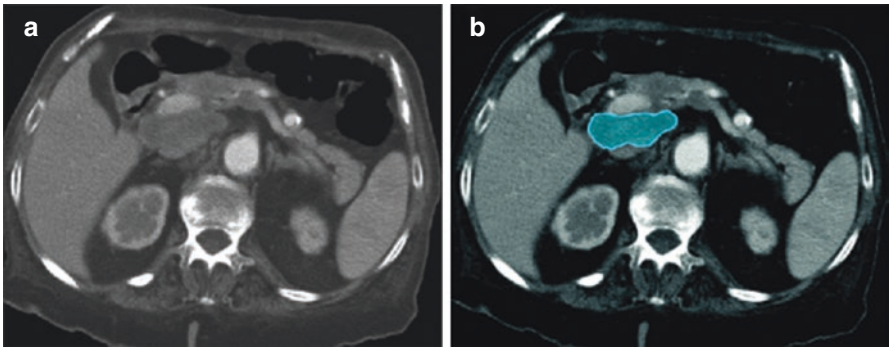

Fig. 3.2 (**a**, **b**) Axial CT image in a patient with hepatoma shows a metastatic low-density portocaval lymph node (blue)

Table 3.2 Size criteria for detecting abdominal malignant lymph nodes [5]

Location	Short axis nodal diameter (mm)
Retrocrural	>6
Paracardiac	>8
Mediastinal	≥10
Gastrohepatic ligament	>8
Upper paraaortic	>9
Portacaval	>10
Portahepatis	>7
Lower paraaortic	>11

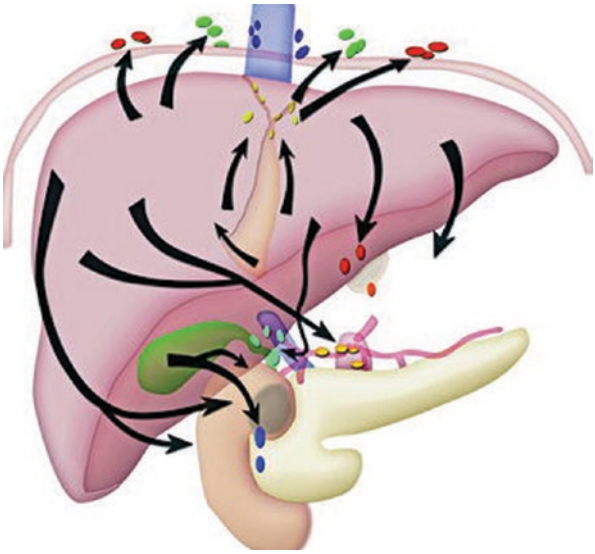

Fig. 3.3 Superficial pathways of lymphatic drainage for the liver. The anterior diaphragmatic nodes consist of the lateral anterior diaphragmatic group and the medial group, which includes the pericardiac nodes and the subxiphoid nodes behind the xiphoid cartilage. The nodes in the falciform ligament drain into the anterior abdominal wall along the superficial epigastric and deep epigastric lymph nodes. The epigastric and the subxiphoid nodes drain into the internal mammary nodes

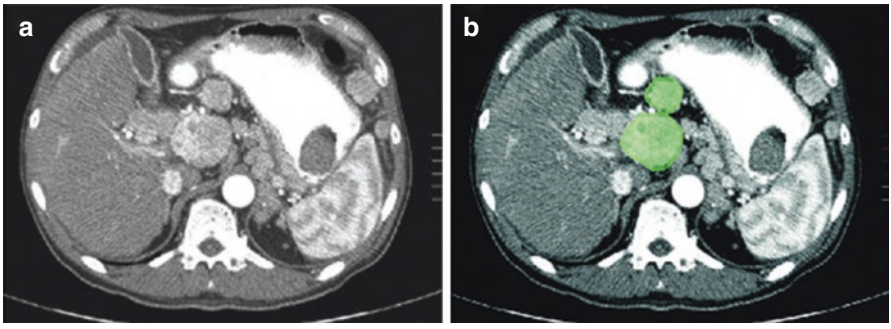

Fig. 3.4 (**a**, **b**) Axial CT image in a patient with hepatocellular carcinoma shows enlarged hypervascular nodes (green) in the periportal locations

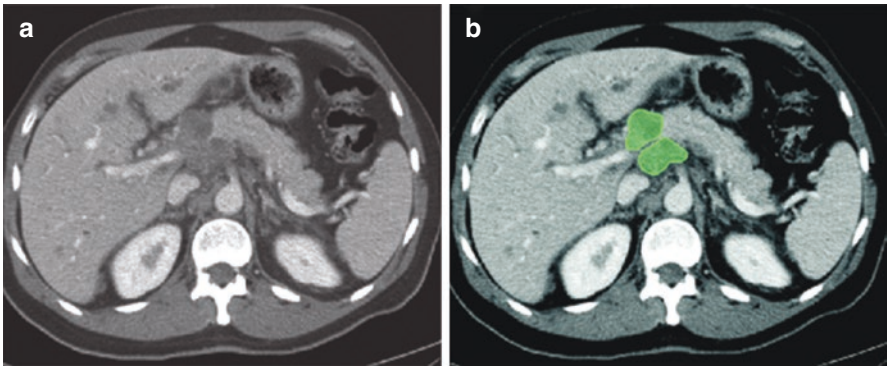

Fig. 3.5 (**a**, **b**) Axial CT image in a patient with hepatoma shows enlarged nodes in the periportal (green) and peripancreatic location causing secondary biliary obstruction

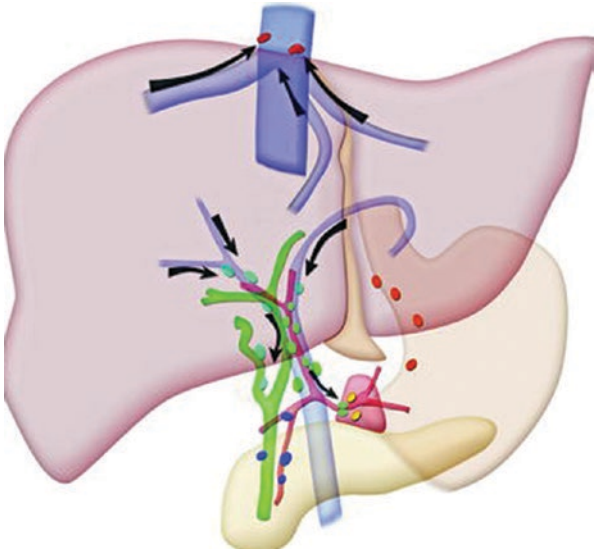

Fig. 3.6 Deep pathways of lymphatic drainage for the liver. The deep pathways follow the hepatic veins to the inferior vena cava nodes and the juxtaphrenic nodes that follow along the phrenic nerve. The pathways that follow the portal vein drain into the hepatic hilar nodes and the nodes in the hepatoduodenal ligament, which then drain into the celiac node and the cisterna chyli

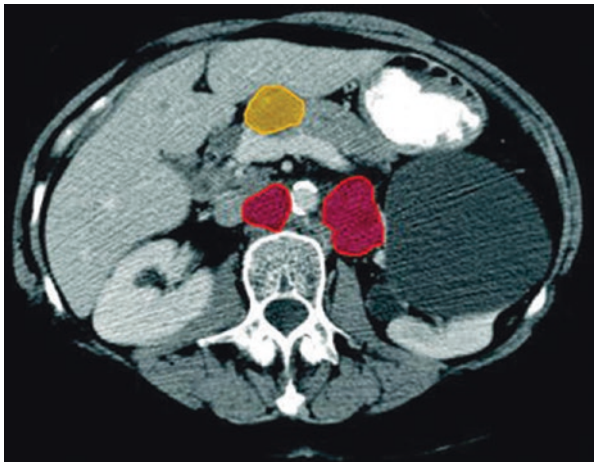

Fig. 3.7 Axial CT image in a patient with cholangiocarcinoma shows enlarged prepancreatic (yellow) and retroperitoneal lymph nodes (red)

Table 3.3 N-stage classification for hepatocellular carcinoma

Stage	Findings
NX	Regional nodes cannot be assessed
N0	No regional nodal metastasis
N1	Metastasis in regional lymph nodes

Table 3.4 Regional lymph nodes for hepatocellular carcinoma [7]

Hepatocellular carcinoma
Hepatoduodenal ligament
Caval lymph nodes
Hepatic artery

3.1.2 Stomach

Gastric cancer is the third most common gastrointestinal malignancy [7]. Lymph node metastasis in gastric cancer is common, and the incidence increases with advanced stages of tumor invasion [21].

The lymphatic drainage of the stomach consists of intrinsic and extrinsic systems (see Fig. 3.8). The intrinsic system includes intramural submucosal and subserosal networks and the extrinsic system forms lymphatic vessels outside the stomach and generally follows the course of the arteries in various peritoneal ligaments around the stomach. These lymphatic vessels drain into the lymph nodes at nodal stations in the corresponding ligaments and drain into the central collecting nodes at the root of the celiac axis and the superior mesenteric artery [1].

Tables 3.5 and 3.6 list the nodal staging for gastric carcinoma and the regional draining lymph nodes. The extent of nodal metastasis as defined by pathologic staging on surgical specimens has been used as prognostic indicators based on the number of positive nodes. However, the nodal groups described in this section are based on anatomic locations according to the Japanese Classification of Gastric Cancer (JCGC).

The JCGC classified the nodes into three groups (see Fig. 3.9):

- Group 1 are lymph nodes around the stomach including the left cardiac, right cardiac, greater and lesser curvature, and supra- and infrapyloric nodes. Resection of these nodes is defined as D1 category (see Fig. 3.10).
- Group 2 are lymph nodes away from the perigastric lymph nodes. They include the left gastric, common hepatic, splenic artery, splenic hilum, proper hepatic, and celiac nodes. Resection of nodes in group 1 and group 2 is defined as D2 category.
- Group 3 are lymph nodes in the hepatoduodenal ligament, posterior pancreas, root of the mesentery, paraesophageal, and diaphragmatic nodes. Resection of the three nodal groups and paraaortic nodes is defined as D3 category.

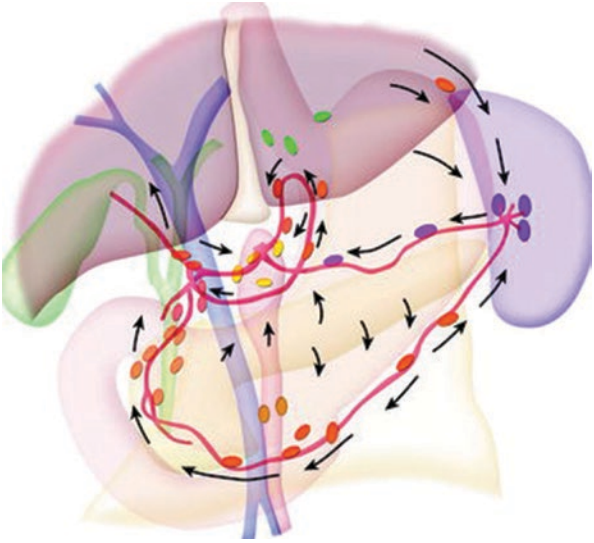

Fig. 3.8 Lymphatic drainage pathways for the stomach

Table 3.5 N-stage classification for gastric cancer

Stage	Findings
NX	Regional lymph node(s) cannot be assessed
N0	No regional lymph node metastasis
N1	Metastasis in 1–6 regional lymph nodes
N2	Metastasis in 7–15 regional lymph nodes
N3	Metastasis in more than 15 regional lymph nodes

Table 3.6 Regional lymph nodes for gastric cancer [7]

Gastric cancer
Greater curvature of stomach
Greater curvature
Greater omental
Gastroduodenal
Gastroepiploic
Pyloric
Pancreaticoduodenal lymph nodes
Pancreatic and splenic area
Pancreaticolienal
Peripancreatic
Splenic
Lesser curvature of stomach
Lesser curvature
Lesser omental
Left gastric
Cardio-esophageal
Common hepatic
Hepatoduodenal ligament

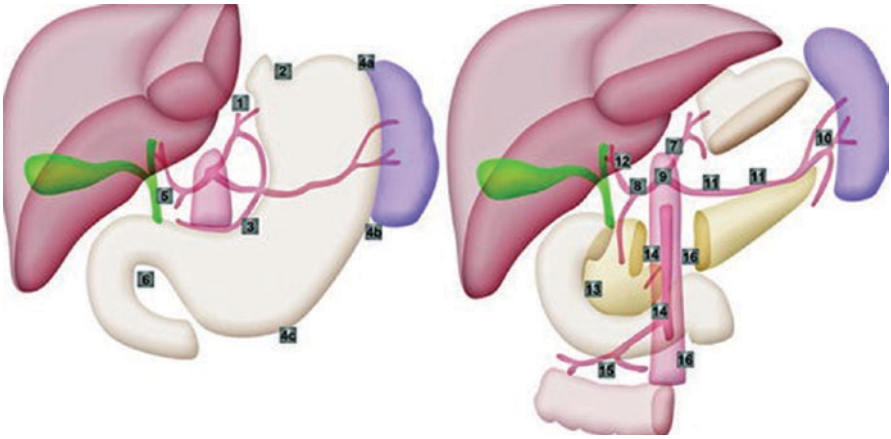

Fig. 3.9 The JCGC classification for perigastric lymph nodes. *Group 1*: *1* right cardial nodes, *2* left cardial nodes, *3* nodes along the lesser curvature, *4* nodes along the greater curvature, *5* suprapyloric nodes, *6* infrapyloric nodes. *Group 2*: *7* nodes along the left gastric artery, *8* nodes along the common hepatic artery, *9* nodes around the celiac axis, *10* nodes at the splenic hilus, *11* nodes along the splenic artery. *Group 3*: *12* nodes in the hepatoduodenale ligament, *13* nodes at the posterior aspect of the pancreas head, *14* nodes at the root of the mesenterium, *15* nodes in the mesocolon of the transverse colon, *16* paraaortic nodes

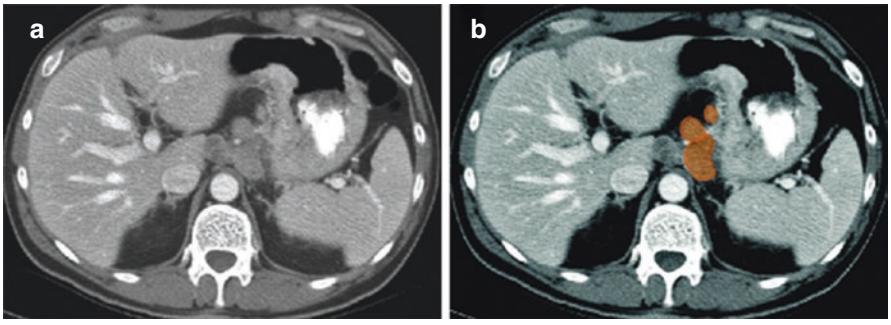

Fig. 3.10 (**a**, **b**) Axial CT image in a patient with gastric carcinoma shows enlarged gastrohepatic lymph nodes (orange) along the lesser curvature

3.1.3 Paraesophageal and Paracardiac Nodes

The lymph from the distal esophagus and the cardiac orifice of the stomach drains to the paraesophageal lymph nodes around the esophagus above the diaphragm and the paracardiac nodes below the diaphragm. They can spread upward along the esophagus to the mediastinal lymph nodes and along the thoracic duct to the left or right supraclavicular nodes or downward along the esophageal branches of the left gastric artery to the left gastric nodes and the celiac nodes (see Fig. 3.11) [1].

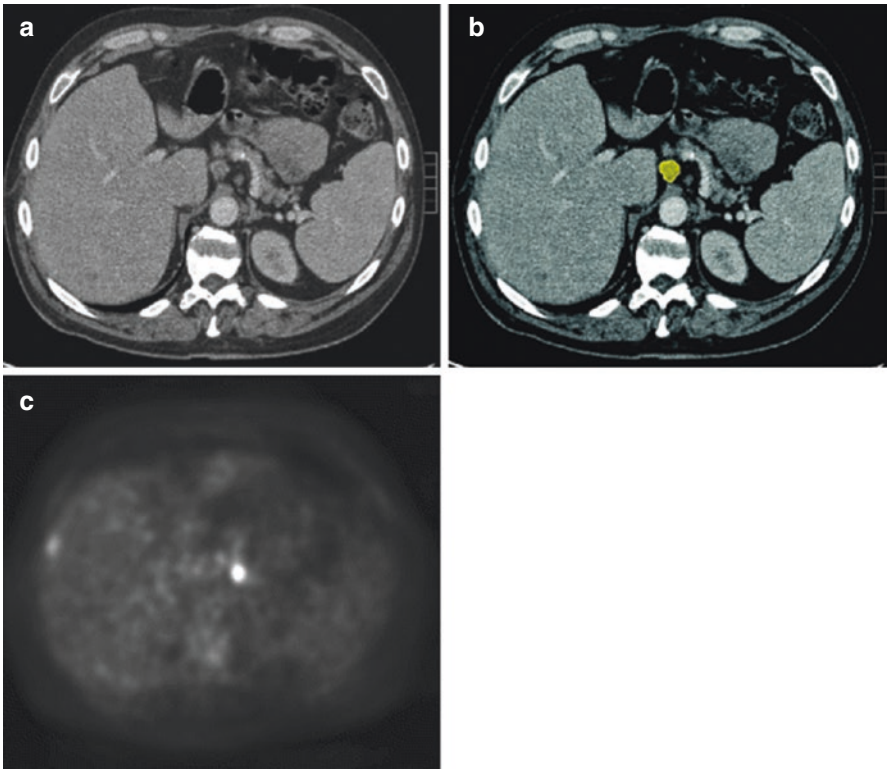

Fig. 3.11 (**a**–**c**) Axial CT image in a patient with esophageal cancer shows enlarged celiac lymph node (yellow). The node shows FDG activity on a PET scan

3.1.4 Nodal Metastases in the Gastrohepatic Ligament

Tumors arising from the area of the stomach along the lesser curvature and the esophagogastric junction, supplied by the left gastric artery, generally metastasize to the lymph nodes in the gastrohepatic ligament (see Fig. 3.12). The primary nodal group (group 1) consists of nodes along the left and right gastric artery anastomosis along the lesser curvature. Group 2 nodes include the nodes along the left gastric artery and vein in the gastropancreatic fold that drain toward the nodes at the celiac axis. Tumors arising from the area of the stomach in the distribution of the right gastric artery along the lesser curvature of the gastric antrum drain into the perigastric nodes and the suprapyloric nodes near the pylorus (group 1). They then drain into the nodes at the common hepatic artery (group 2), from where the right gastric artery originates or the area where the right gastric vein drains into the portal vein. From these nodes, drainage continues along the hepatic artery toward the celiac axis (group 2). The lymphatic anastomoses in the gastrohepatic ligament along the lesser curvature form the alternate drainage pathways for the tumors arising from this region. Less commonly they are involved in pancreatic cancer due to retrograde tumor extension from the celiac nodes [1].

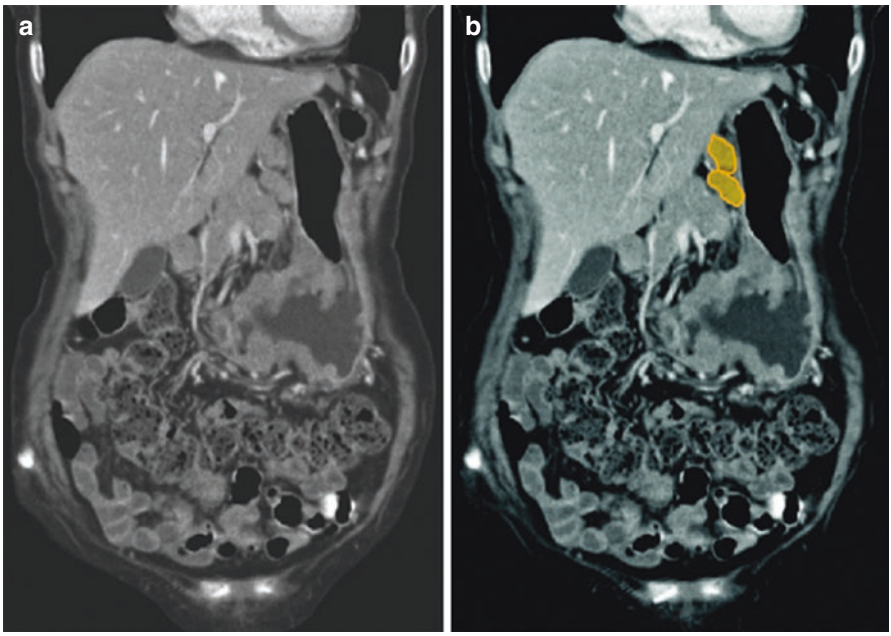

Fig. 3.12 (**a**, **b**) Coronal reformatted CT image in a patient with stomach cancer show prominent gastrohepatic ligament lymph nodes (orange)

3.1.5 Nodal Metastases in the Gastrosplenic Ligament

Lymphatic drainage of tumors at the posterior wall and the greater curvature of the gastric fundus spreads to the perigastric nodes (group 1) in the superior segment of the gastrosplenic ligament, then follows along the branches of the short gastric artery to the nodes at the hilum of the spleen (group 2). The tumors from the greater curvature of the body of the stomach also spread to the perigastric nodes (group 1) and then advance along the left gastroepiploic vessels and drain into the lymph nodes in the splenic hilum (group 2). From the splenic hilum, they may spread to the nodes along the splenic artery to the nodes at the celiac axis (group 2). In addition, the tumors from the posterior wall of the gastric fundus and upper segment of the body may drain along the posterior gastric artery to the nodes along the splenic artery that are known as the suprapancreatic nodes or the nodes in the splenorenal ligament and then to the nodes at the celiac axis [1].

3.1.6 Nodal Metastases in the Gastrocolic Ligament

Primary tumors involving the greater curvature of the antrum of the stomach in the distribution of the right gastroepiploic artery spread to the perigastric nodes (group 1) accompanying the right gastroepiploic vessels that course along the greater curvature of the stomach. They drain into the nodes at the gastrocolic trunk (group 2)

(see Fig. 3.13) or the nodes at the origin of the right gastroepiploic artery and the nodes along the gastroduodenal artery (the subpyloric or infrapyloric node). From there, they may proceed to the celiac axis or the root of the superior mesenteric artery [1].

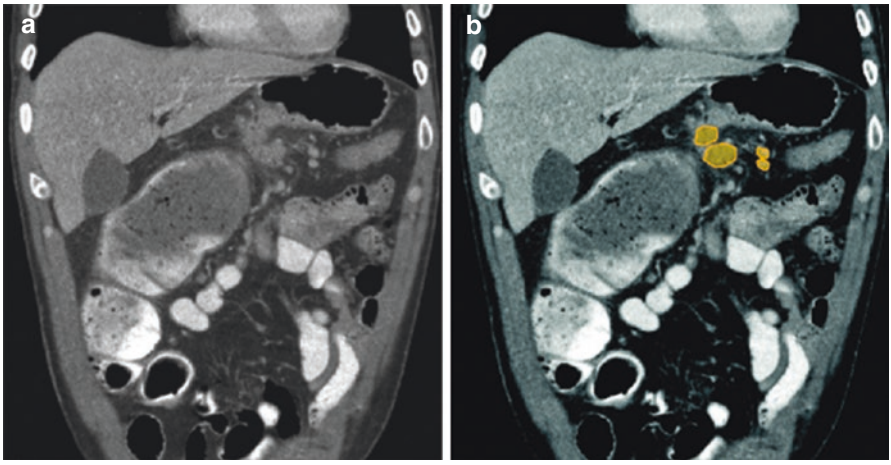

Fig. 3.13 (**a**, **b**) Coronal reformatted CT image in a patient with stomach cancer shows prominent gastrocolic ligament lymph nodes (orange)

3.1.7 Inferior Phrenic Nodal Pathways

Tumors involving the esophagogastric junction or the gastric cardia may invade the diaphragm as they penetrate beyond its wall. The lymphatic drainage of the peritoneal surface of the diaphragm is via the nodes along the inferior phrenic artery and veins that course along the left crus of the diaphragm toward the celiac axis or the left renal vein [1].

CT is the most widely recommended method for preoperative staging of gastric cancer with sensitivities for lymph node staging ranging from approximately 63% to 92% [22]. The presence of lymph node metastases precludes endoscopic resection in cases of T1 tumor that would otherwise be eligible [23]. Involvement of regional nodes also affects the extent of lymphadenectomy and the need for chemotherapy. Group one nodal involvement implies subserosal spread of disease and excludes patients from laparascopic gastrectomy [23, 24].

The variable nodal drainage pattern with skip metastases and the presence of metastatic disease in normal-sized nodes, however, continue to be challenging [24]. The accuracy of MRI is considered to be inferior to CT for examining LN involvement but may be more accurate than CT for nonnodal metastatic disease [25]. Further diagnostic imaging via 18 F-fluoro-deoxy-D-glucose (FDG) PET is not a replacement for CT in gastric cancer cases but can complement CT for staging and prognostic information [26].

3.1.8 Small Intestine

The three most common malignant tumors of the small intestine are lymphoma, adenocarcinoma, and carcinoid tumor. The path of regional nodal metastasis follows the vessels of the involved segment to the root of the superior mesentery artery (SMA) (see Fig. 3.14) near the head of the pancreas and to the extra peritoneum [1].

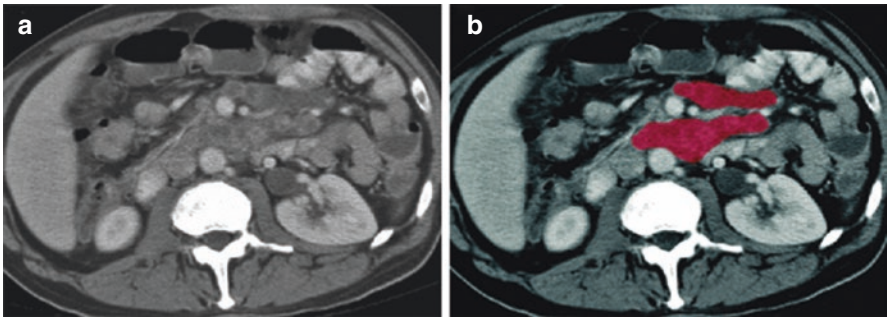

Fig. 3.14 (**a**, **b**) Axial CT image in a patient with lymphoma shows enlarged, clustered mesenteric root lymph nodes (red)

3.1.9 Appendix

Similar to the small intestine, carcinoid tumor, noncarcinoid epithelial tumor, and lymphoma are the three most common tumors of the appendix. Lymph node metastasis is rare in the tumors of the appendix. Generally, nodal metastasis follows the ileocolic vessels along the root of the mesentery to the origin of the SMA and the paraaortic region [1].

3.1.10 Colorectal

Colorectal adenocarcinoma is the third most common cancer and the third most common cause of cancer deaths [7]. Lymph node metastasis is one of the most important prognostic factors in the TNM classification—defining the number of positive nodes in stepwise incremental groups—that correlates with poorer outcome (Table 3.7) (see Fig. 3.15) [1]. Patients with node-negative disease have 5-year survival rates of 70–80% compared to 30–60% in those with node-positive disease [27].

Accurate identification of abnormal lymph nodes is important as it aids in preoperative planning of the extent of surgery. Patients with T1–T2 rectal tumors can be treated with resection alone. If there are nodal metastases (or if the tumor is T3), neoadjuvant treatment is required. It also helps in identifying regions of possible recurrence in treated cases, in the clinical setting of increasing carcinoembryonic antigen levels [3, 28, 29].

Table 3.8 lists regional lymph nodes for colorectal cancer. Lymph from the wall of the large intestine and rectum drains into the lymph nodes accompanying the arteries and veins of the corresponding colon and rectum [2, 3]. The nodes can be classified according to the location as follows (see Fig. 3.16).

- The epicolic nodes accompanying the vasa recta outside the wall
- The paracolic nodes along the marginal vessels
- The intermediate mesocolic nodes along the ileocolic, right colic, middle colic, left ascending and descending colic, left colic, and sigmoidal arteries
- The principal nodes at the gastrocolic trunk, the origin of the middle colic artery, and the origin of the inferior mesenteric artery

Cecum and ascending colon. The lymphatic drainage is via the epicolic nodes and the paracolic nodes, which are seen in proximity with the marginal vessels along the mesocolic side of the colon. From the paracolic nodes (see Fig. 3.17), lymphatic drainage follows the vessels in the ileocolic (see Fig. 3.18) and right colic mesentery, where the intermediate nodal group is located and drains into the principal nodes at the root of the SMA.

Transverse colon. The lymphatic drainage is from the epicolic nodes and the paracolic nodes (along the marginal vessels) to the intermediate nodal group situated along the middle colic vessels and then into the principal node at the root of the SMA (see Fig. 3.19).

Left side of colon and upper rectum. The lymphatic drainage is from the epicolic and the paracolic (along the marginal vessels) group to the intermediate mesocolic nodes including the left colic nodes and then to the principal inferior mesenteric artery (IMA) nodes (see Fig. 3.20).

Lower rectum. There are two different lymphatic pathways: one is along the superior hemorrhoidal vessels toward the mesorectum (see Figs. 3.21, 3.22, 3.23, and 3.24) and mesocolon; the other is the lateral route, along the middle and inferior hemorrhoidal vessels toward the hypogastric and obturator nodes and then to the paraaortic nodes (see Figs. 3.25 and 3.26).

Anus. Anal tumors usually spread to the superficial inguinal nodes and then to the deep inguinal nodes along the common femoral vessels. From here they ascend to the external iliac, common iliac, and paraaortic groups (see Figs. 3.27 and 3.28). Table 3.9 demonstrates the most recent TNM staging for anal carcinoma.

A key pathologic characteristic in determining the stage of disease in colon cancer is the status of the draining lymph nodes [30]. The criteria for distance between tumor and mesorectal fascia in case of T3 tumors also apply for mesorectal nodes lying within the mesorectal fat (see Fig. 3.29). Nodes are more than 3 mm in size, whereas tumor deposits are smaller. If lymph nodes are involved with tumor (stage III disease), 5-fluorouracil–based adjuvant therapy improves survival [31]. However, for node-negative disease (stage II disease), the benefits of adjuvant chemotherapy are not well established.

MRI with the use of ultrasmall superparamagnetic iron oxide (USPIO) contrast agents has been shown to increase the diagnostic specificity of the nodal assessment compared to size and morphology on conventional MRI. This is of particular value in identifying patients with node-negative disease who are being considered for local excision surgery [32].

Because of the nonspecificity on anatomic imaging, additional imaging studies and aspiration biopsy are frequently used to establish the diagnosis of metastatic disease before treatment decision. In primary rectal cancer, PET-CT has been shown to be useful in identifying patients achieving complete response to chemoradiotherapy. It has the potential to identify patients who would benefit from surveillance rather than radical resection [33].

Table 3.7 N-stage classification for colorectal cancer

Stage	Findings
NX	Regional nodes cannot be assessed
N1	Metastasis in one to three regional lymph nodes
N2	Metastasis in four or more regional lymph nodes

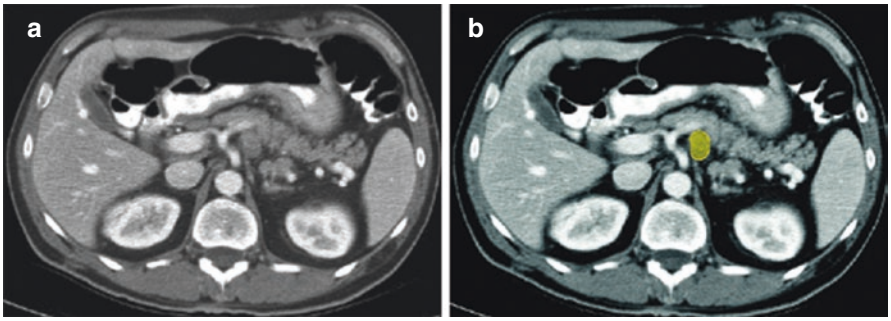

Fig. 3.15 (**a**, **b**) Axial CT image in a patient with primary colon cancer shows an enlarged celiac lymph node (yellow)

Table 3.8 Regional lymph nodes for colorectal cancer [7]

Colorectal cancer
Pericolic/perirectal
Ileocolic
Right colic
Middle colic
Left colic
Inferior mesenteric artery
Superior rectal (hemorrhoidal)

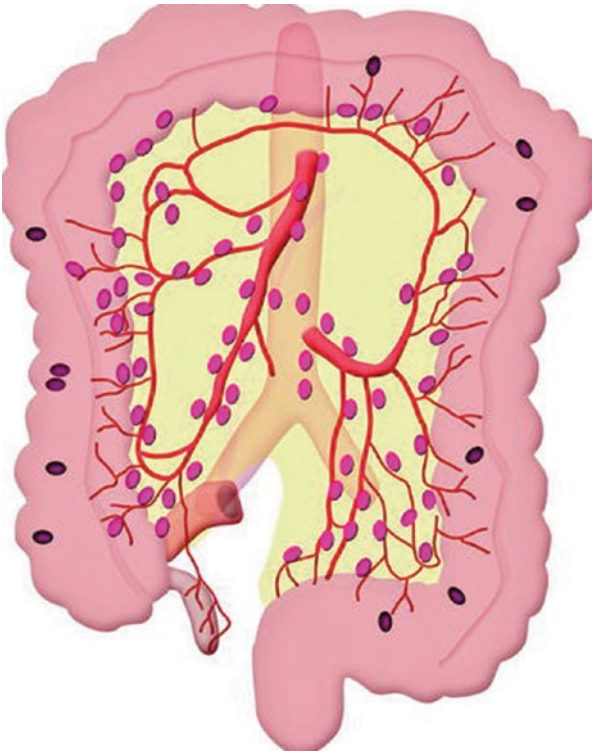

Fig. 3.16 Lymphatic drainage pathways for the colon

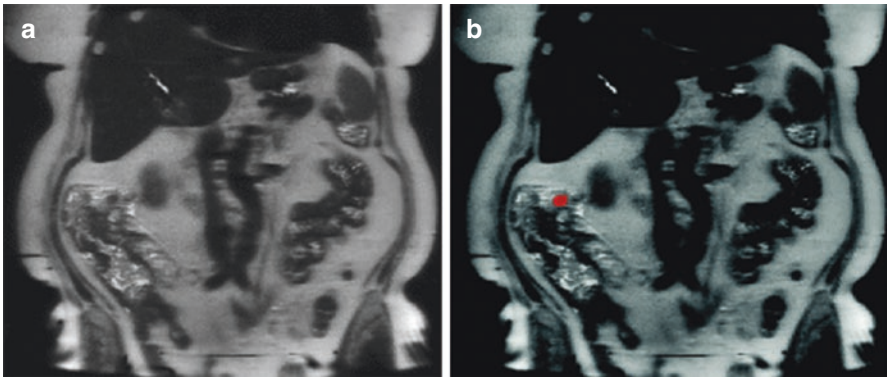

Fig. 3.17 (**a**, **b**) Coronal T2-weighted image in a patient with ascending colon adenocarcinoma with metastatic pericolic lymph node (red)

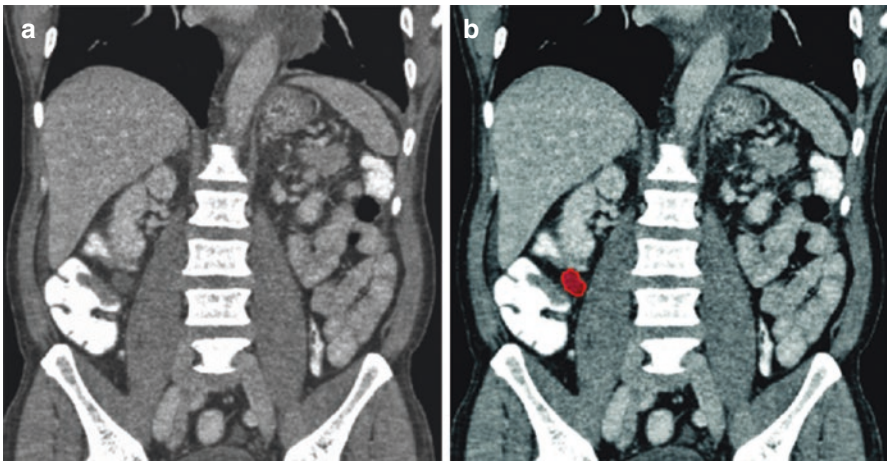

Fig. 3.18 (**a**, **b**) Coronal reformatted CT image in a patient with cecal cancer shows prominent ileocolic lymph node (red)

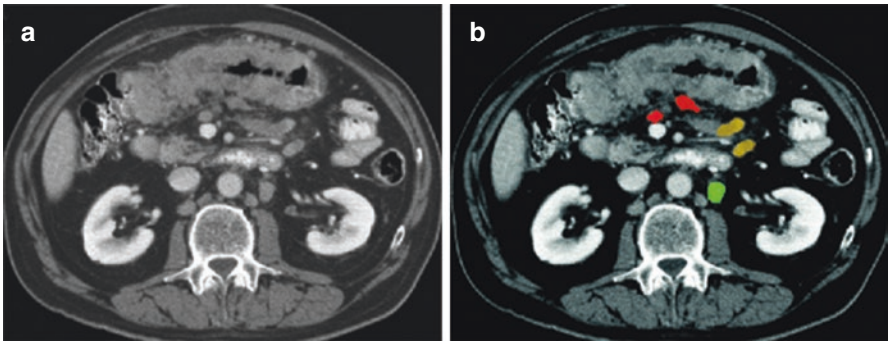

Fig. 3.19 (**a**, **b**) Axial CT image in a patient with malignancy in the transverse colon shows pericolonic (red), mesenteric (yellow), and left periaortic (green) lymph nodes

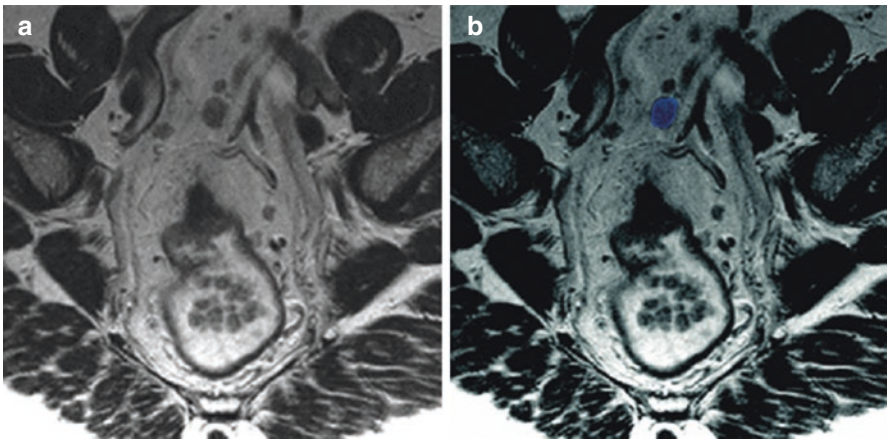

Fig. 3.20 (**a**, **b**) Axial oblique T2-weighted images in a patient with rectal cancer shows metastatic inferior mesenteric lymph node (blue)

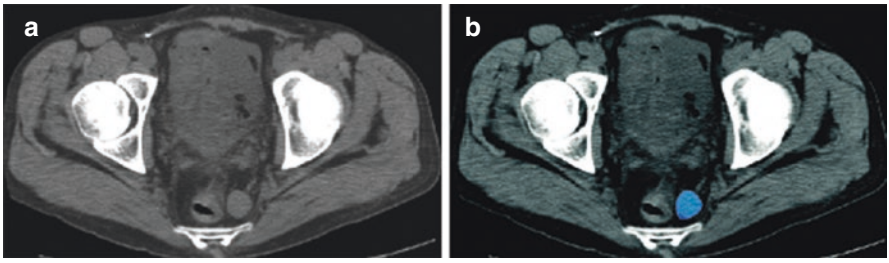

Fig. 3.21 (**a**, **b**) Axial CT image in a patient with primary rectal cancer shows an enlarged left perirectal lymph node (blue)

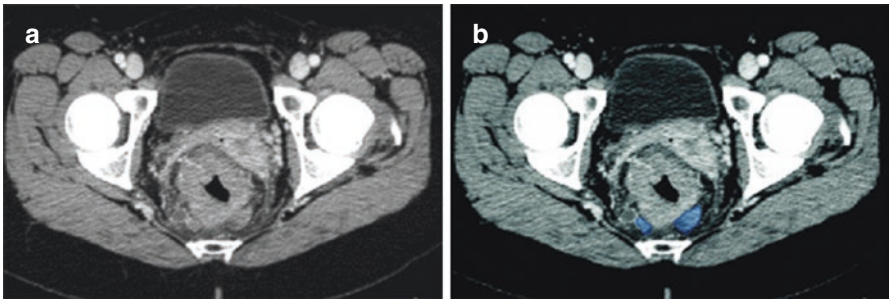

Fig. 3.22 (**a**, **b**) Axial CT image in a patient with rectal cancer showing metastatic perirectal lymph nodes (blue)

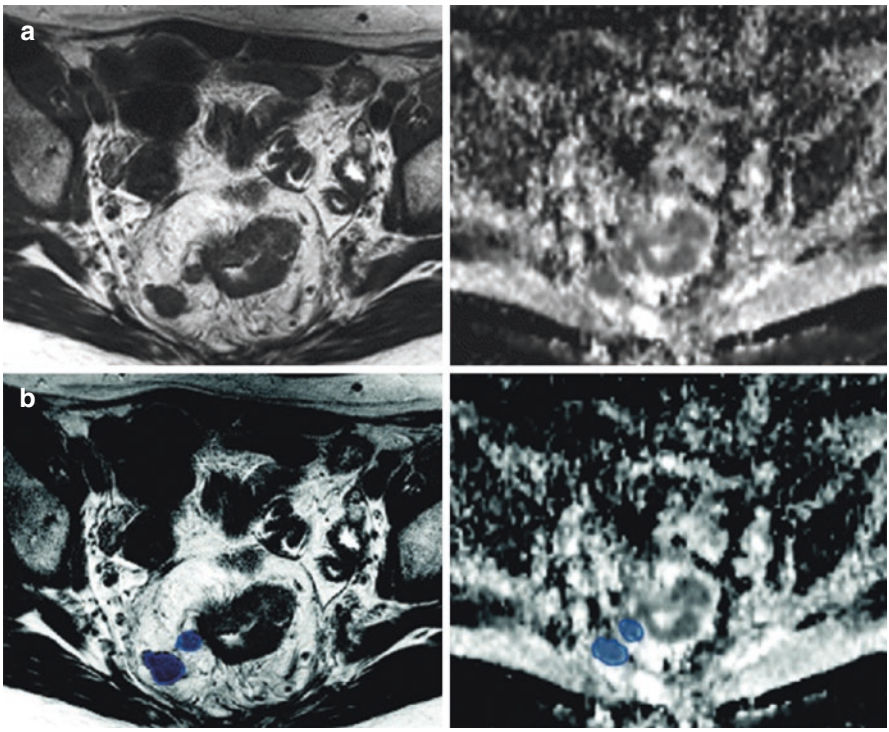

Fig. 3.23 (**a**, **b**) Axial T2-weighted image (left) and Apparent Diffusion Coefficient (ADC) map (right) of a patient with rectal cancer showing metastatic perirectal lymph nodes (blue) with restricted diffusion and dark signal on ADC

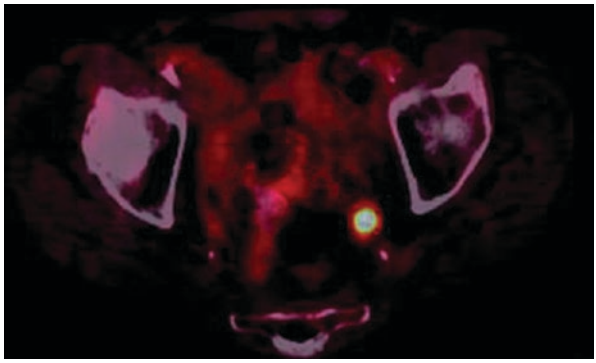

Fig. 3.24 Fused axial PET-CT image shows FDG avid metastatic left perirectal lymph node

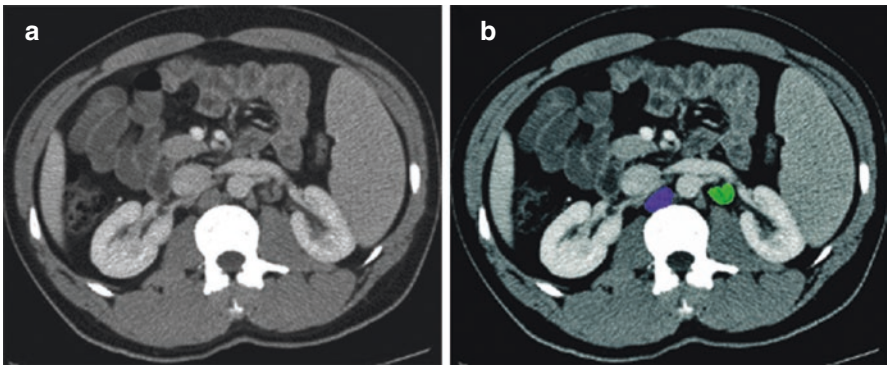

Fig. 3.25 (**a**, **b**) Axial CT image in a patient with rectal cancer (not shown) shows metastatic retrocaval (purple) and left periaortic lymph node (green)

Fig. 3.26 Coronal reformatted CT image in a patient with primary colonic mucinous adenocarcinoma shows calcified metastatic left periaortic lymph nodes (arrows)

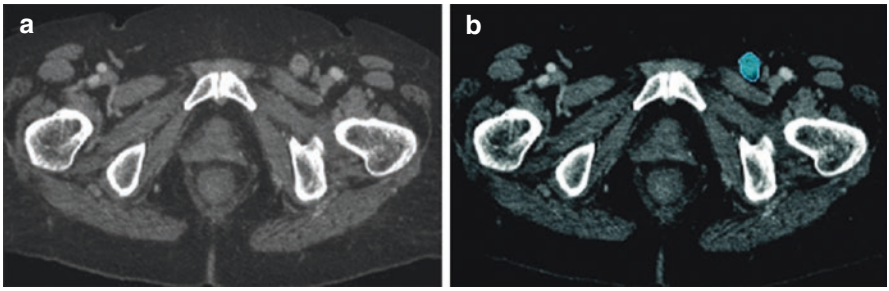

Fig. 3.27 (**a**, **b**) Axial CT image in a patient with anal cancer shows metastatic left inguinal lymph node (blue)

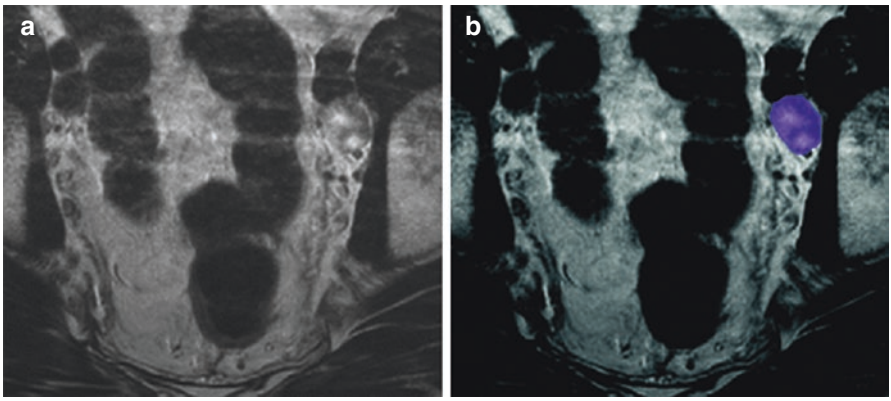

Fig. 3.28 (**a**, **b**) Axial T2-weighted image in a patient with anal cancer shows metastatic left external iliac lymph node (purple)

Table 3.9 Regional lymph nodes for anal carcinoma

Stage	Findings
N0	No regional lymph node metastasis
N1	Metastasis in regional lymph node(s)
N1a	Metastases in inguinal, mesorectal, and/or internal iliac nodes
N1b	Metastases in external iliac nodes
N1c	Metastases in external iliac and in inguinal, mesorectal, and/or internal iliac nodes

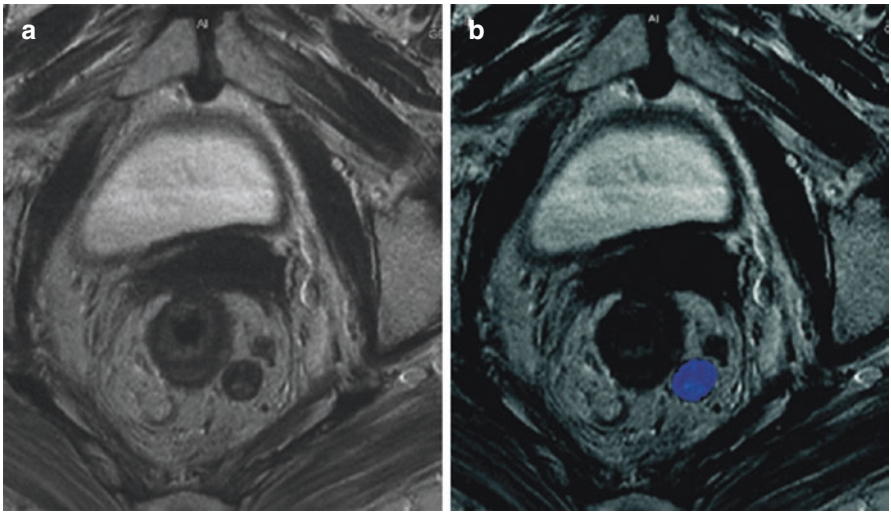

Fig. 3.29 (**a**, **b**) Axial T2-weighted image in a patient with rectal cancer shows heterogenous metastatic perirectal lymph node (blue)

3.2 Retroperitoneal Lymph Nodes

3.2.1 Renal, Upper Urothelial, and Adrenal Malignancies

Lymphatics draining the kidney are derived from three plexuses: one beneath the renal capsule, the second around the renal tubules, and the third in the perirenal fat. These plexuses drain into lymphatic trunks that run from the renal hilum along the renal vein to the paraaortic nodes, which then drain into the cisterna chyli and predominantly the left supraclavicular nodes via the thoracic duct. The lymphatic drainage for the proximal ureters is to the paraaortic nodes in the region of the renal vessels and gonadal artery. The middle ureteral lymphatics drain to the common iliac nodes and the lower ureteral lymphatics to the external and internal iliac nodes. All the iliac nodes drain to the paraaortic nodes, cisterna chyli, and predominantly the left supraclavicular nodes via the thoracic duct. The adrenal lymphatics drain to the paraaortic nodes [1].

3.2.2 Lymphatic Spread of Malignancies

3.2.2.1 Renal Tumor

Renal tumors account for 3% of all cancer cases and deaths [34]; the majority of these are renal cell carcinomas. Lymph node status is a strong prognostic indicator in patients with kidney cancer [35, 36] with 5-year disease-specific survival for patients with node-positive disease reported between 21% and 38% [1, 2, 37]. Patients without lymph node involvement however (N0) have a 5-year estimated survival of greater than 50% [38].

Lymphatic spread of renal cell carcinomas (RCC) is initially to regional lymph nodes. These include nodes along the renal arteries from the renal hilum to the paraaortic nodes at this level (see Fig. 3.30). The presence of lymph node involvement in RCC doubles a patient's risk of distant metastasis [3]. Ten to fifteen percent of patients have regional nodal involvement without distant spread. Lymphatic spread may continue above or below the level of the renal hilum, with subsequent spread to the cisterna chyli and to the left supraclavicular nodes via the thoracic duct. Occasionally, there is spread from these nodes to the mediastinum and pulmonary hilar nodes [1].

Table 3.9 lists the N-Stage classification for kidney cancer. Diagnosis of pathologic lymph nodes is problematic, as approximately 50% of enlarged regional nodes are hyperplastic [39]. Criteria currently used for suspect nodes are those 1 cm or more in short axis and loss of oval shape and fatty hilus. Clustering of three or more nodes in the regional area is also suggestive of metastatic spread.

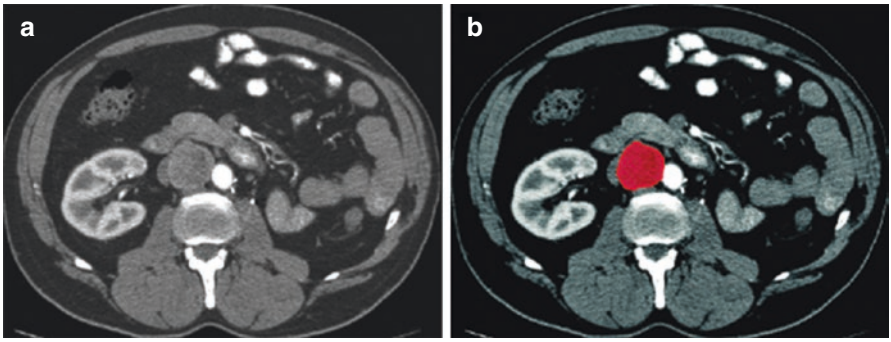

Fig. 3.30 (**a**, **b**) Axial CT image in a patient with left nephrectomy for renal cell cancer shows enlarged aortocaval (red) lymph node with biopsy-proven recurrent RCC

3.2.2.2 Urothelial Tumors

Periureteral extension from ureteral transitional cell carcinoma (TCC) is secondary to growth through the ureteral wall and involvement of the extensive lymphatic drainage. The sites of regional lymphatic spread are dependent on the location of the tumor. The paraaortic nodes are involved initially in the renal pelvic and upper ureteral tumors (see Fig. 3.31). If the origin is from the middle ureter, metastases are to the common iliac nodes, whereas lower ureteral tumors involve the internal and external nodes initially. The iliac nodes drain into the paraaortic nodes. Lymphatics within the wall of the ureter allow for direct extension within the wall [1].

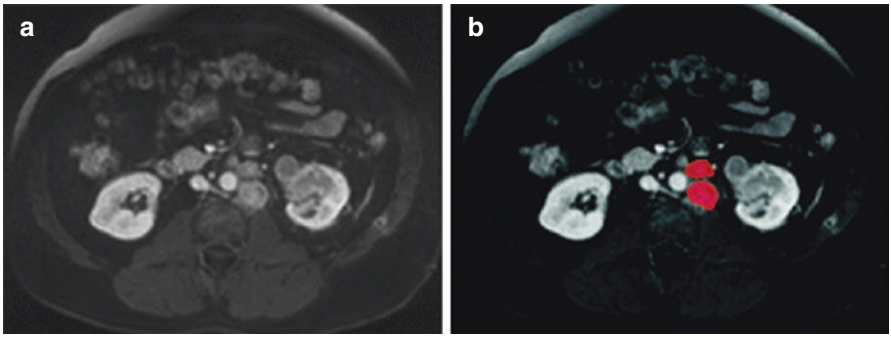

Fig. 3.31 (**a**, **b**) Axial post gadolinium-enhanced T1-weighted image shows metastatic left periaortic lymph nodes (red) in a patient with left transitional cell carcinoma

3.2.2.3 Adrenal Tumors

Primary malignant tumors of the adrenal gland arise from the cortex as adrenocortical carcinomas or from the medulla as pheochromocytomas or in the spectrum of the neuroblastoma ganglioneuroma complex. Most of these tumors spread by lymphatic spread to the paraaortic lymph nodes [1].

3.3 Pancreatic Cancer

Pancreatic cancer is the second most common gastrointestinal malignancy and is the fifth leading cause of cancer-related death. The majority of cases are ductal adenocarcinomas (exocrine ductal epithelium, 95% of cases). Up to two-thirds may be located in the head of the pancreas. Lymph node metastases are common in pancreatic and duodenal cancer and they carry a poor prognosis [40, 41].

3.3.1 Lymphatic Spread and Nodal Metastasis

Lymphatic drainage of the head of the pancreas is different from that of the body and tail (Tables 3.10 and 3.11; see Fig. 3.32).

The head of the pancreas and the duodenum share similar drainage pathways by following arteries around the head of the pancreas [41, 42]. They can be divided into three major routes: the gastroduodenal, the inferior pancreaticoduodenal, and the dorsal pancreatic:

1. Around the head of the pancreas, multiple lymph nodes can be found between the pancreas and duodenum above and below the root of the transverse mesocolon and anterior and posterior to the head of the pancreas. Although many names are used for these nodes such as the inferior and superior pancreaticoduodenal

nodes (see Fig. 3.33), they can be designated peripancreatic nodes (see Fig. 3.34). The gastroduodenal route collects lymphatics from the anterior pancreaticoduodenal nodes (see Figs. 3.35, 3.36, and 3.37), which drain lymphatics along the anterior surface of the pancreas, and the posterior pancreaticoduodenal nodes, which follow the bile duct along the posterior pancreaticoduodenal vein to the posterior periportal node.
2. The inferior pancreaticoduodenal route also receives lymphatic drainage from the anterior and posterior pancreaticoduodenal nodes by following the inferior pancreaticoduodenal artery to the superior mesenteric artery node. Occasionally, they may also drain into the node at the proximal jejunal mesentery.
3. The dorsal pancreatic route is uncommon. It collects lymphatics along the medial border of the head of the pancreas and follows the branch of the dorsal pancreatic artery to the superior mesenteric artery or celiac node. The lymphatic drainage of the body and tail of the pancreas follows the dorsal pancreatic artery, the splenic artery, and vein to the celiac lymph node.

The lymphatic drainage of the body and tail of the pancreas follows the dorsal pancreatic artery, the splenic artery, and vein to the celiac lymph node. The nodal staging for pancreatic cancer based on American Joint Committee on Cancer (AJCC) criteria is listed in Tables 3.12 and 3.13. Table 3.14 lists the regional lymph nodes for pancreatic cancer.

Preoperative imaging studies, using the size of the nodes as diagnostic criteria, are not accurate for the diagnosis of nodal metastasis. Normal-sized lymph nodes may harbor micrometastases, whereas enlarged nodes are often reactive [43]. Because of the lack of accuracy, peripancreatic lymph nodes and the nodes along the gastroduodenal artery and inferior pancreaticoduodenal artery are included in radiation field, and they are routinely resected at the time of pancreaticoduodenectomy. However, it is important to note when an abnormal node, such as one with low density and/or irregular border, is detected beyond the usual drainage basin and outside the routine surgical or radiation field, such as in the proximal jejunal mesentery or at the base of the transverse mesocolon, as these can be the sites of recurrent disease [1].

Currently, the only potentially curative therapy for pancreatic carcinoma is complete surgical resection; however, only 5–20% of patients have potentially resectable disease at the time of diagnosis [44]. With regard to nodal staging, the distinction of regional versus extraregional nodes is crucial to identify. Abnormal nodes that are in the surgical bed are considered nodal metastasis and are generally not a contraindication to surgery. If, however, they are confirmed at surgery, adjuvant chemotherapy is indicated [45]. For cancers in the pancreatic head/neck, this includes lymph nodes along the celiac axis and in the peripancreatic and periportal regions, and for cancers in the body/tail, this includes lymph nodes along the common hepatic artery (CHA), celiac axis, splenic artery, and splenic hilum. Involved nodes outside the surgical bed are considered distant metastases and surgery is contraindicated [45].

For patients with suspected cancer recurrence, PET/CT has been shown to improve the diagnostic accuracy, especially in patients with elevated tumor markers

but equivocal CT findings [46]. PET-CT also has a potential use for radiotherapy treatment planning by more accurately depicting the burden of gross tumor volume compared to CT alone [47].

Table 3.10 N-stage classification for renal cancer

Stage	Findings
NX	Regional nodes cannot be assessed
N0	No regional nodal metastases
N1	Metastases in a single regional lymph node
N2	Metastasis in more than one regional lymph node

Table 3.11 Lymph node groups in tumors of the pancreatic head, body, and tail

Lymph node station group	Tumor of head	Tumor of body/tail
1	13a, 13b, 17a, 17b	8a, 8p, 10, 11p, 11d, 18
2	6, 8a, 8p, 12a, 12b, 12p, 14p, 14d	7, 9, 14p, 14d, 15
3	1, 2, 3, 4, 5, 7, 9, 10, 11p, 11d, 15, 16a2, 16bl, 18	5, 6, 12a, 12b, 12p, 13a, 13b, 17a, 17b, 16a2, 16b1

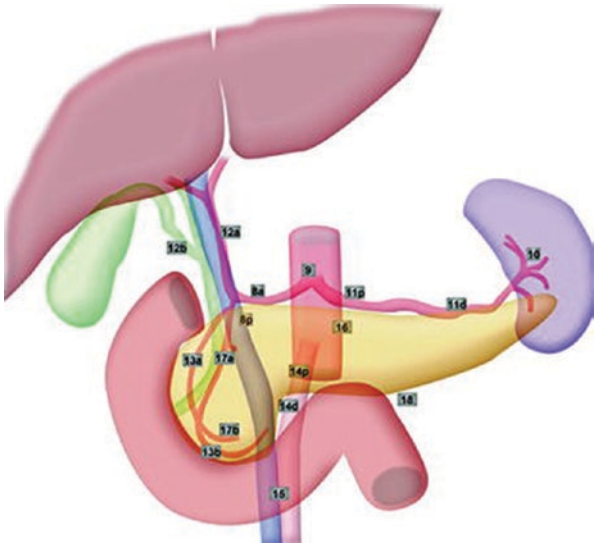

Fig. 3.32 Lymph node stations according to the classification of pancreatic carcinoma proposed by the Japan Pancreas Society (see Table 3.11)

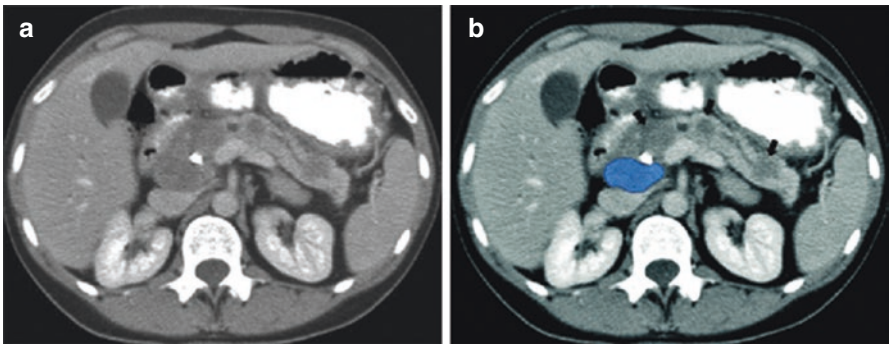

Fig. 3.33 (**a**, **b**) Axial CT image in a patient with metastatic sarcoma with multiple metastases to the pancreas (arrows) and to the superior pancreaticoduodenal lymph node (blue)

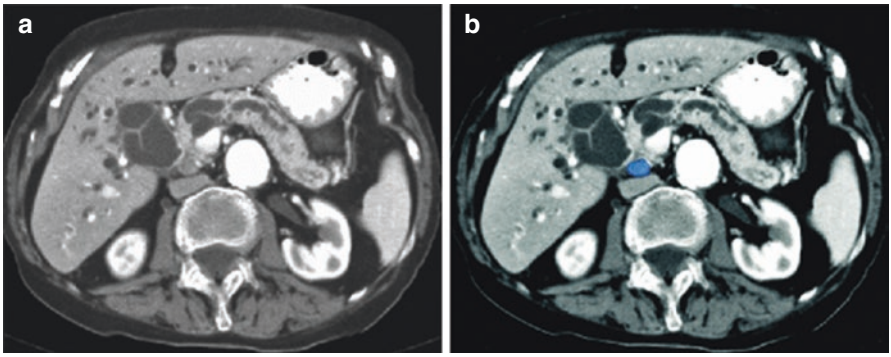

Fig. 3.34 (**a**, **b**) Axial CT image in a patient with primary pancreatic adenocarcinoma shows metastatic retropancreatic lymph node (blue)

Fig. 3.35 Axial CT image in a patient with healed tuberculosis shows a calcified lymph node in superior pancreaticoduodenal location

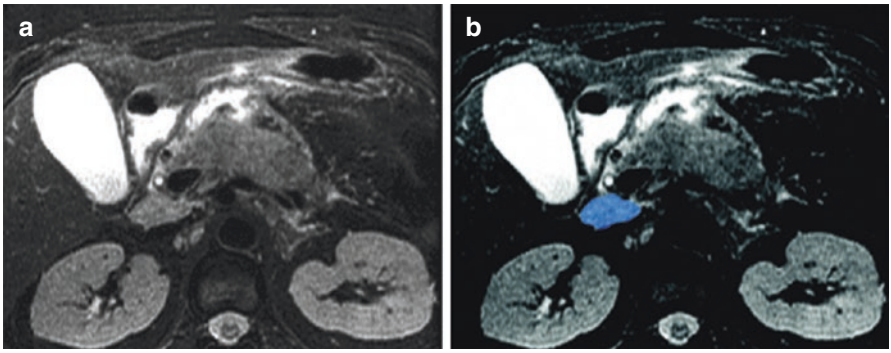

Fig. 3.36 (**a**, **b**) Axial T2-weighted image in a patient with pancreatitis shows an enlarged superior pancreaticoduodenal lymph node (blue)

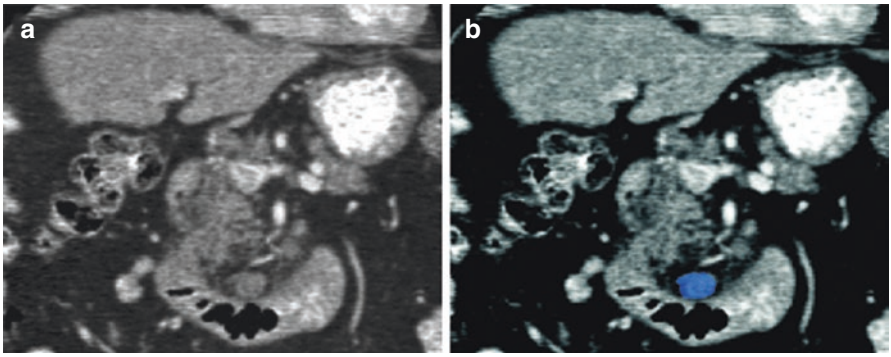

Fig. 3.37 (**a**, **b**) Coronal reformatted image in a patient with primary pancreatic adenocarcinoma (not shown) shows a prominent inferior pancreaticoduodenal lymph node (blue)

Table 3.12 Lymph node stations in pancreatic carcinoma as proposed by the Japan Pancreas Society

Station	Name
1	Right cardial lymph nodes
2	Left cardial lymph nodes
3	Lymph nodes along the lesser curvature of the stomach
4	Lymph nodes along the greater curvature of the stomach
5	Suprapyloric lymph nodes
6	Infrapyloric lymph nodes
7	Lymph nodes along the left gastric artery
8a	Lymph nodes in the anterosuperior group along the common hepatic artery
8p	Lymph nodes in the posterior group along the common hepatic artery
9	Lymph nodes around the celiac artery
10	Lymph nodes at the splenic hilum
11p	Lymph nodes along the proximal splenic artery

(continued)

Table 3.12 (continued)

Station	Name
11d	Lymph nodes along the distal splenic artery
12a	Lymph nodes along the hepatic artery
12p	Lymph nodes along the portal vein
12b	Lymph nodes along the bile duct
13a	Lymph nodes on the posterior aspect of the superior portion of the head of the pancreas
13b	Lymph nodes on the posterior aspect of the inferior portion of the head of the pancreas
14p	Lymph nodes on the proximal superior mesenteric artery
14d	Lymph nodes along the distal superior mesenteric artery
15	Lymph nodes along the middle colic artery
16	Lymph nodes around the abdominal aorta
16a1	Lymph nodes around the aortic hiatus of the diaphragm
16b1	Lymph nodes around the abdominal aorta (from the superior margin of the celiac trunk to the inferior margin of the inferior mesenteric artery)
16b2	Lymph nodes around the abdominal aorta (from the superior margin of the inferior mesenteric artery to the aortic bifurcation)
17a	Lymph nodes on the anterior surface of the superior portion of the head of the pancreas
17b	Lymph nodes on the anterior surface of the inferior portion of the head of the pancreas
18	Lymph nodes along the inferior margin of the pancreas

Table 3.13 N-stage classification for pancreatic cancer

Stage	Findings
NX	Regional nodes cannot be assessed
N0	No regional nodal metastases
N1	Regional lymph node metastasis

Table 3.14 The regional lymph nodes for pancreatic cancer

Pancreatic cancer
Peripancreatic
Hepatic artery
Celiac axis
Pyloric
Splenic region

References

1. Meyers MA, et al. Meyers' dynamic radiology of the abdomen: normal and pathologic anatomy. 6th ed. New York: Springer-Verlag; 2011.
2. McDaniel KP, Charnsangavej C, DuBrow RA, Varma DG, Granfield CA, Curley SA. Pathways of nodal metastasis in carcinomas of the cecum, ascending colon, and transverse colon: CT demonstration. AJR Am J Roentgenol. 1993;161(1):61–4. https://doi.org/10.2214/ajr.161.1.8517322.
3. Granfield CA, Charnsangavej C, Dubrow RA, Varma DG, Curley SA, Whitley NO, et al. Regional lymph node metastases in carcinoma of the left side of the colon and rectum: CT demonstration. AJR Am J Roentgenol. 1992;159(4):757–61. https://doi.org/10.2214/ajr.159.4.1529837.
4. Gest TPP. Anatomy: medcharts. New York: Iloc; 1994.
5. Dorfman RE, Alpern MB, Gross BH, Sandler MA. Upper abdominal lymph nodes: criteria for normal size determined with CT. Radiology. 1991;180(2):319–22. https://doi.org/10.1148/radiology.180.2.2068292.
6. Dodd GD, Baron RL, Oliver JH, Federle MP, Baumgartel PB. Enlarged abdominal lymph nodes in end-stage cirrhosis: CT-histopathologic correlation in 507 patients. Radiology. 1997;203(1):127–30. https://doi.org/10.1148/radiology.203.1.9122379.
7. Morón FE, Szklaruk J. Learning the nodal stations in the abdomen. Br J Radiol. 2007;80(958):841–8. https://doi.org/10.1259/bjr/64292252.
8. Harisinghani MG, et al. Noninvasive detection of clinically occult lymph-node metastases in prostate cancer. N Engl J Med. 2003;348(25):2491–9. https://doi.org/10.1056/NEJMoa022749.
9. Mao Y, Hedgire S, Harisinghani M. Radiologic assessment of lymph nodes in oncologic patients. Curr Radiol Rep. 2013;2(2):36. https://doi.org/10.1007/s40134-013-0036-6.
10. Neuwelt A, Sidhu N, Hu C-AA, Mlady G, Eberhardt SC, Sillerud LO. Iron-based superparamagnetic nanoparticle contrast agents for MRI of infection and inflammation. AJR Am J Roentgenol. 2015;204(3):W302–13. https://doi.org/10.2214/AJR.14.12733.
11. Gauthé M, et al. Role of fluorine 18 fluorodeoxyglucose positron emission tomography/computed tomography in gastrointestinal cancers. Dig Liver Dis. 2015;47(6):443–54. https://doi.org/10.1016/j.dld.2015.02.005.
12. Harisinghani MG, et al. Ferumoxtran-10-enhanced MR lymphangiography: does contrast-enhanced imaging alone suffice for accurate lymph node characterization? AJR Am J Roentgenol. 2006;186(1):144–8. https://doi.org/10.2214/AJR.04.1287.
13. Frija J, Bourrier P, Zagdanski AM, De Kerviler E. Diagnosis of a malignant lymph node. J Radiol. 2005;86(2 Pt 1):113–25. https://doi.org/10.1016/s0221-0363(05)81331-9.
14. Egner JR. AJCC cancer staging manual. JAMA. 2010;304(15):1726–7. https://doi.org/10.1001/jama.2010.1525.
15. Kobayashi S, et al. Surgical treatment of lymph node metastases from hepatocellular carcinoma. J Hepato-Biliary-Pancreat Sci. 2011;18(4):559–66. https://doi.org/10.1007/s00534-011-0372-y.
16. Xia F, et al. Positive lymph node metastasis has a marked impact on the long-term survival of patients with hepatocellular carcinoma with extrahepatic metastasis. PLoS One. 2014;9(4):e95889. https://doi.org/10.1371/journal.pone.0095889.
17. Pan T, et al. Percutaneous CT-guided radiofrequency ablation for lymph node oligometastases from hepatocellular carcinoma: a propensity score–matching analysis. Radiology. 2016;282(1):259–70. https://doi.org/10.1148/radiol.2016151807.
18. Clark HP, Carson WF, Kavanagh PV, Ho CPH, Shen P, Zagoria RJ. Staging and current treatment of hepatocellular carcinoma. Radiographics. 2005;25(Suppl 1):S3–23. https://doi.org/10.1148/rg.25si055507.
19. Kalogeridi M-A, et al. Role of radiotherapy in the management of hepatocellular carcinoma: a systematic review. World J Hepatol. 2015;7(1):101–12. https://doi.org/10.4254/wjh.v7.i1.101.

20. Wu H, Liu S, Zheng J, Ji G, Han J, Xie Y. Transcatheter arterial chemoembolization (TACE) for lymph node metastases in patients with hepatocellular carcinoma. J Surg Oncol. 2015;112(4):372–6. https://doi.org/10.1002/jso.23994.
21. Hartgrink HH, et al. Extended lymph node dissection for gastric cancer: who may benefit? Final results of the randomized Dutch gastric cancer group trial. J Clin Oncol. 2004;22(11):2069–77. https://doi.org/10.1200/JCO.2004.08.026.
22. Smyth EC, Verheij M, Allum W, Cunningham D, Cervantes A, Arnold D. Gastric cancer: ESMO Clinical Practice Guidelines for diagnosis, treatment and follow-up†. Ann Oncol. 2016;27:v38–49. https://doi.org/10.1093/annonc/mdw350.
23. Japanese Gastric Cancer Association. Japanese gastric cancer treatment guidelines 2014 (ver. 4). Gastric Cancer. 2017;20(1):1–19. https://doi.org/10.1007/s10120-016-0622-4.
24. Young JJ, et al. Ligaments and lymphatic pathways in gastric adenocarcinoma. Radiographics. 2019;39(3):668–89. https://doi.org/10.1148/rg.2019180113.
25. Dicken BJ, Bigam DL, Cass C, Mackey JR, Joy AA, Hamilton SM. Gastric adenocarcinoma: review and considerations for future directions. Ann Surg. 2005;241(1):27–39. https://doi.org/10.1097/01.sla.0000149300.28588.23.
26. Coburn NG. Lymph nodes and gastric cancer. J Surg Oncol. 2009;99(4):199–206. https://doi.org/10.1002/jso.21224.
27. Ong MLH, Schofield JB. Assessment of lymph node involvement in colorectal cancer. World J Gastrointest Surg. 2016;8(3):179–92. https://doi.org/10.4240/wjgs.v8.i3.179.
28. Taylor FGM, Swift RI, Blomqvist L, Brown G. A systematic approach to the interpretation of preoperative staging MRI for rectal cancer. Am J Roentgenol. 2008;191(6):1827–35. https://doi.org/10.2214/AJR.08.1004.
29. Steup WH, Moriya Y, van de Velde CJH. Patterns of lymphatic spread in rectal cancer. A topographical analysis on lymph node metastases. Eur J Cancer. 2002;38(7):911–8. https://doi.org/10.1016/s0959-8049(02)00046-1.
30. Rajput A, et al. Meeting the 12 lymph node (LN) benchmark in colon cancer. J Surg Oncol. 2010;102(1):3–9. https://doi.org/10.1002/jso.21532.
31. Wolpin BM, Meyerhardt JA, Mamon HJ, Mayer RJ. Adjuvant treatment of colorectal cancer. CA Cancer J Clin. 2007;57(3):168–85. https://doi.org/10.3322/canjclin.57.3.168.
32. Koh D-M, et al. Diagnostic accuracy of nodal enhancement pattern of rectal cancer at MRI enhanced with ultrasmall superparamagnetic iron oxide: findings in pathologically matched mesorectal lymph nodes. Am J Roentgenol. 2010;194(6):W505–13. https://doi.org/10.2214/AJR.08.1819.
33. Pozo ME, Fang SH. Watch and wait approach to rectal cancer: a review. World J Gastrointest Surg. 2015;7(11):306–12. https://doi.org/10.4240/wjgs.v7.i11.306.
34. American Cancer Society. Cancer facts & figures 2020. https://www.cancer.org/research/cancer-facts-statistics/all-cancer-facts-figures/cancer-facts-figures-2020.html. Accessed 11 Oct 2020.
35. Karakiewicz PI, et al. Tumor size improves the accuracy of TNM predictions in patients with renal cancer. Eur Urol. 2006;50(3):521–8; discussion 529. https://doi.org/10.1016/j.eururo.2006.02.034.
36. Lughezzani G, et al. Prognostic significance of lymph node invasion in patients with metastatic renal cell carcinoma: a population-based perspective. Cancer. 2009;115(24):5680–7. https://doi.org/10.1002/cncr.24682.
37. Capitanio U, et al. Stage-specific effect of nodal metastases on survival in patients with non-metastatic renal cell carcinoma. BJU Int. 2009;103(1):33–7. https://doi.org/10.1111/j.1464-410X.2008.08014.x.
38. Tadayoni A, Paschall AK, Malayeri AA. Assessing lymph node status in patients with kidney cancer. Transl Androl Urol. 2018;7(5):766–73. https://doi.org/10.21037/tau.2018.07.19.
39. Israel GM, Bosniak MA. Renal imaging for diagnosis and staging of renal cell carcinoma. Urol Clin North Am. 2003;30(3):499–514. https://doi.org/10.1016/s0094-0143(03)00019-3.

40. Takahashi T, Ishikura H, Motohara T, Okushiba S, Dohke M, Katoh H. Perineural invasion by ductal adenocarcinoma of the pancreas. J Surg Oncol. 1997;65(3):164–70. https://doi.org/10.1002/(sici)1096-9098(199707)65:3<164::aid-jso4>3.0.co;2-4.
41. Kayahara M, Nakagawara H, Kitagawa H, Ohta T. The nature of neural invasion by pancreatic cancer. Pancreas. 2007;35(3):218–23. https://doi.org/10.1097/mpa.0b013e3180619677.
42. Pawlik TM, et al. Prognostic relevance of lymph node ratio following pancreaticoduodenectomy for pancreatic cancer. Surgery. 2007;141(5):610–8. https://doi.org/10.1016/j.surg.2006.12.013.
43. Wong JC, Raman S. Surgical resectability of pancreatic adenocarcinoma: CTA. Abdom Imaging. 2010;35(4):471–80. https://doi.org/10.1007/s00261-009-9539-2.
44. Laeseke PF, Chen R, Jeffrey RB, Brentnall TA, Willmann JK. Combining in vitro diagnostics with in vivo imaging for earlier detection of pancreatic ductal adenocarcinoma: challenges and solutions. Radiology. 2015;277(3):644–61. https://doi.org/10.1148/radiol.2015141020. Accessed 5 Oct 2020.
45. Pietryga JA, Morgan DE. Imaging preoperatively for pancreatic adenocarcinoma. J Gastrointest Oncol. 2015;6(4):343–57. https://doi.org/10.3978/j.issn.2078-6891.2015.024.
46. Cameron K, et al. Recurrent pancreatic carcinoma and cholangiocarcinoma: 18F-fluorodeoxyglucose positron emission tomography/computed tomography (PET/CT). Abdom Imaging. 2011;36(4):463–71. https://doi.org/10.1007/s00261-011-9729-6.
47. Parlak C, Topkan E, Onal C, Reyhan M, Selek U. Prognostic value of gross tumor volume delineated by FDG-PET-CT based radiotherapy treatment planning in patients with locally advanced pancreatic cancer treated with chemoradiotherapy. Radiat Oncol. 2012;7(1):37. https://doi.org/10.1186/1748-717X-7-37.